Accepted Manuscript

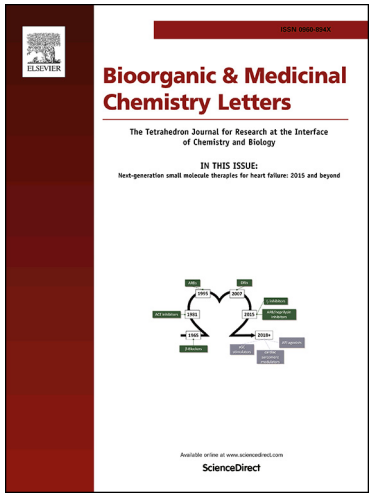

Structural development of 1H-pyrazolo-[3,4-b]pyridine-4-carboxylic acid derivatives as human peroxisome proliferator-activated receptor alpha (PPAR α)-selective agonists

Hiroyuki Miyachi, Tomohiro Yuzuriha, Ryotaro Tabata, Syohei Fukuda, Kazuto Nunomura, Bangzhong Lin, Tadayuki Kobayashi, Kenji Ishimoto, Takefumi Doi, Keisuke Tachibana

PII: S0960-894X(19)30444-5
DOI: https://doi.org/10.1016/j.bmcl.2019.06.062
Reference: BMCL 26540

To appear in: *Bioorganic & Medicinal Chemistry Letters*

Received Date: 16 May 2019
Revised Date: 19 June 2019
Accepted Date: 29 June 2019

Please cite this article as: Miyachi, H., Yuzuriha, T., Tabata, R., Fukuda, S., Nunomura, K., Lin, B., Kobayashi, T., Ishimoto, K., Doi, T., Tachibana, K., Structural development of 1H-pyrazolo-[3,4-b]pyridine-4-carboxylic acid derivatives as human peroxisome proliferator-activated receptor alpha (PPAR α)-selective agonists, *Bioorganic & Medicinal Chemistry Letters* (2019), doi: https://doi.org/10.1016/j.bmcl.2019.06.062

Structural development of 1*H*-pyrazolo-[3,4-b]pyridine-4-carboxylic acid derivatives as human peroxisome proliferator-activated receptor alpha (PPARα)-selective agonists

Hiroyuki Miyachi[a,1*], Tomohiro Yuzuriha[b,2], Ryotaro Tabata[b], Syohei Fukuda[b], Kazuto Nunomura[b], Bangzhong Lin[b], Tadayuki Kobayashi[b], Kenji Ishimoto[b], Takefumi Doi[b], Keisuke Tachibana[b]

[a] Graduate School of Medicine, Dentistry and Pharmaceutical Sciences, Okayama University, 1-1-1, Tsushima-Naka, Kita-ku, Okayama 700-8530, Japan.

[1] (Current address) Lead Exploration Unit, Drug Discovery Initiative, The University of Tokyo, 7-3-1 Hongo, Bunkyo-ku, Tokyo 113-0033, Japan.

[b] Graduate School of Pharmaceutical Sciences, Osaka University, 1-6 Yamadaoka, Suita, Osaka 565-0871, Japan.

[2] (Current address) Faculty of Pharmaceutical Sciences, Setsunan University, 45-1 Nagaotoge-cho, Hirakata, Osaka 573-0101, Japan.

Abstract— We previously reported that 1*H*-pyrazolo-[3,4-b]pyridine-4-carboxylic acid derivative **6** is an agonist of human peroxisome proliferator-activated receptor alpha (hPPARα). Here, we prepared a series of 1*H*-pyrazolo-[3,4-b]pyridine-4-carboxylic acid derivatives in order to examine the structure-activity relationships (SAR). SAR studies clearly indicated that the steric bulkiness of the substituent on 1*H*-pyrazolo-[3,4-b]pyridine ring, the position of the distal hydrophobic tail part, and the distance between the distal hydrophobic tail part and the acidic head part are critical for hPPARα agonistic activity. These SAR results are somewhat different from those reported for fibrate-class hPPARα agonists. A representative compound (**10f**) was as effective as fenofibrate in reducing the elevated plasma triglyceride levels in a high-fructose-fed rat model.

Peroxisome proliferator-activated receptors (PPARs) are members of the human nuclear receptor family, functioning as ligand-dependent transcription factors with pleiotropic biological functions that include regulatory roles in lipid, lipoprotein and glucose homeostasis. PPARs are activated by various kinds of endogenous saturated and unsaturated fatty acids and their metabolites, as well as by synthetic ligands.[1] Three subtypes have been isolated to date: PPARα (NR1C1), PPARδ (NR1C2) and PPARγ (NR1C3). Among these subtypes, hPPARα is mostly expressed in tissues involved in lipid oxidation, such as liver, kidney, and regulates genes involved in uptake and oxidation of free fatty acids, triglyceride hydrolysis; it also up-regulates reverse cholesterol transport.[2] Fibrate-class antihyperlipidemic agents, such as fenofibrate (**1**) which effectively lower elevated serum triglycerides and moderately increase high-density lipoproteins (HDL), can bind and activate hPPARα. However, their affinity is weak (in the high micromolar range), and the subtype selectivity is not high.[3] Recently, a selective hPPARα modulator (SPPARMα), pemafibrate was launched as a hypolipidemic agent in Japan.

We have been engaged in structural development studies of ligands for nuclear receptors, including PPAR subtypes, and have reported some hPPARα-selective agonists, such as compounds **4** and **5** (APHM-13).[4, 5] We also solved the X-ray crystallographic structure of **5** complexed with the hPPARα ligand-binding domain (LBD).[6] In addition, we recently discovered a new structural class of hPPARα agonist (**6**), whose basic structure, i.e., 1*H*-pyrazolo[3,4-b]pyridine-4-carboxylic acid, is different from those of known fibrate-class hPPARα agonists, using our established screening system of human hepatoblastoma cell lines with luciferase reporter expression driven by promoters containing peroxisome proliferator-responsive elements (PPREs) together with tetracycline-regulated expression of full-length hPPARα (relative hPPARα transactivation activity of **6** to the DMSO control was 150.83± 27.71 at 1 μM

).[7] As an extension of that work, we describe here the preparation of a series of 1*H*-pyrazolo-[3,4-b]pyridine-4-carboxylic acid derivatives in order to examine the structure-activity relationships (SAR) for hPPARα-agonistic activity.

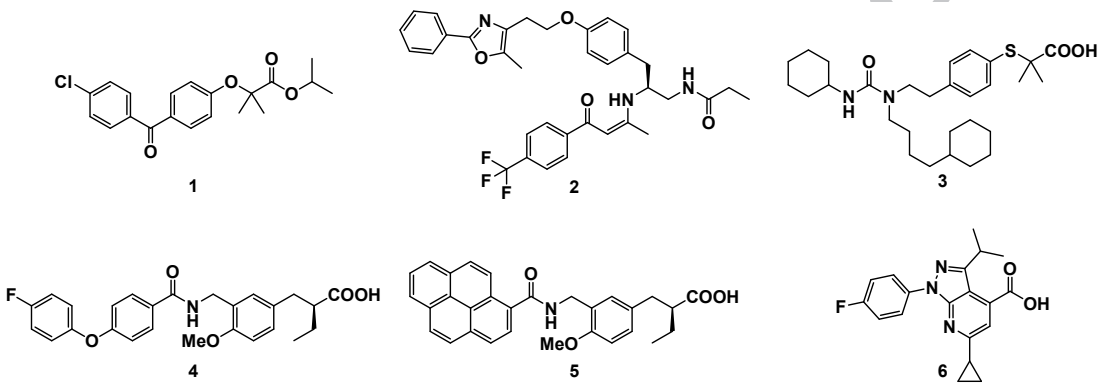

Figure 1. The chemical structures of hPPARα agonists fenofibrate (**1**), GW-7647 (**3**), our reported compounds **4**, APHM-13 (**5**), and **6**, and hPPARα antagonist GW-6471 (**2**).

The synthetic routes to the present series of 1*H*-pyrazolo-[3,4-b]pyridine-4-carboxylic acid derivatives are outlined in Scheme 1. Compounds **10a-10ae** were prepared from methyl ester derivative (**7**) in 4 steps. Methyl ester derivative (**7**) was treated with acetonitrile in the presence of sodium hydride as a base, followed by reaction with aryl hydrazine to afford the corresponding 1*H*-pyrazol-5-amine derivative (**8**). 1*H*-Pyrazolo-[3,4-b]pyridine ring formation was performed by the reaction of **8** with α,γ-diketoester in acetic acid, and subsequent alkaline

hydrolysis afforded the desired **10a-10ae**. To confirm the structures of these compounds, we performed X-ray crystallographic analysis of the precursor ethyl ester derivative of **10f** (CCDC 1900468; an ORTEP drawing is shown in the box in Scheme 1).

1*H*-Pyrazolo-[3,4-b]pyridine-5-carboxylic acid derivative **14** was prepared from **11**. Michael addition of **11** with diethyl ethoxymethylene malonate afforded the adduct **12**, which was treated with phosphoryl chloride followed by alkaline hydrolysis to afford **14**.

A hybrid-type compound of **4** and **10** was prepared from **10p**. The carboxyl group of **10p** was reduced with BH_3-THF, then oxidized with activated MnO_2 to afford the formyl derivative **15**, which was treated with triethyl 2-phosphonobutyrate, followed by hydrogenolysis and alkaline hydrolysis to afford the desired product **17**.

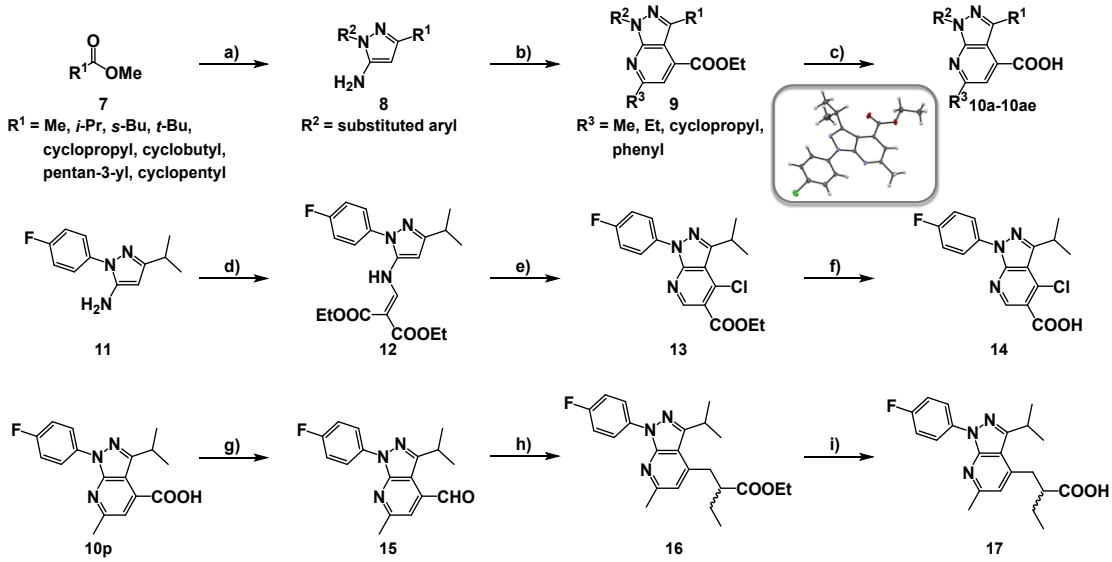

Scheme 1. Synthetic routes to the present series of compounds. Reagents and conditions: a) (1) NaH, MeCN, THF reflux, 2 h, (2) arylhydrazines, EtOH, cHCl, 160˚C, 50 min (microwave), 35-70% (2 steps); b) $R^3COCH_2COCOOEt$, AcOH, 170˚C, 50 min (microwave), 63-90%; c) 1 mol/L NaOH, EtOH, reflux, overnight, 48-95%; d) diethyl ethoxymethylene malonate, EtOH, reflux, overnight, 80%; e) $POCl_3$, reflux, overnight, 48%; f) 1 mol/L NaOH, EtOH, r.t., overnight, 90-95%; g) (1) BH_3-THF, THF, reflux, 10 h, 85%; (2) MnO_2, CH_2Cl_2, r.t., overnight, 90%; h) (1) $(EtO)_2POCH(Et)CO_2Et$, NaH, THF r.t., overnight, 76%, (2) H_2, 10% Pd−C, EtOH, r.t., quant.; i) 1 mol/L NaOH, EtOH, r.t., overnight, 90%.

Considering the hydrophobic nature of the large binding pocket of the hPPAR LBD,[8] we prepared 1*H*-pyrazolo-[3,4-b]pyridine derivatives with various hydrophobic substituents at the R^1, R^2 and R^3 positions depicted in Table 1. Broadly speaking, the steric bulkiness of the substituent introduced at the R^1 position, the position of the acidic carboxyl group and the distance between R^2 substituent and the 4-position carboxyl group each greatly affected hPPARα transactivation activity. In the case of a smaller R^1 substituent such as a methyl group or cyclopropyl group (**10a**, **10b**), the hPPARα transactivation activity was very weak. However, compounds with an isopropyl group at the R^1 position (**10c-10r**, except **10s**) exhibited similar or greater hPPARα transactivation activity compared with 10 μM fenofibrate. Cyclobutyl and cyclopentyl substitution at the R^1 position (**10t**, **10y-10aa**) also resulted in comparable hPPARα transactivation activity to fenofibrate, while pentan-3-yl substitution (**10ab-10ae**) resulted in more potent activity. However, compounds with a *tert*-butyl group at the R^1 position (**10u, 10v**) did not show significant hPPARα transactivation activity.

In the case of the R^2 substituent, a phenyl group is preferable, while the pyridine derivative (**10s**) did not show hPPARα transactivation activity in our assay system. This result is interesting, but at present we cannot explain it. As for substituted phenyl groups at R^2, the steric factor may again be important, because the order of activity for halogen-substituted phenyl groups was F < Cl > Br = I. The fact that the 3-benzyloxy derivative (**10e**) was less active is consistent with this idea.

The optimum location of the acidic head carboxyl group might be the 4-position, as the 5-carboxyl derivative (**14**) exhibited poor hPPARα transactivation activity. Surprisingly, 2-ethylphenyl propanoic acid derivative (**17**), which is a mimic of compounds **4** and **5**, showed less hPPARα transactivation activity.

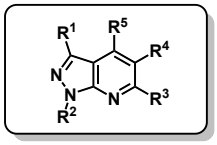

No.	R^1	R^2	R^3	R^4	R^5	relative activity	SD	EC_{50} (μM)
		DMSO				0.00		
		fenofibrate (1)				100.00		
		GW-7647 (3)				199.64	43.09	
		6				150.83	27.71	
10a	Me	phenyl	Me	H	COOH	13.62	0.56	N.T.
10b	cyclopropyl	4-Cl-phenyl	Me	H	COOH	24.56	6.15	N.T.
10c	i-Pr	3-Cl-phenyl	Me	H	COOH	96.72	35.20	N.T.
10d	i-Pr	4-CF_3-phenyl	Me	H	COOH	26.02	5.18	N.T.
10e	i-Pr	3-BnO-phenyl	Me	H	COOH	47.42	7.03	N.T.
10f	i-Pr	4-Cl-phenyl	Me	H	COOH	187.37	36.03	0.66
10g	i-Pr	4-Cl-phenyl	Et	H	COOH	195.94	44.69	1.39
10h	i-Pr	4-Cl-phenyl	cyclopropyl	H	COOH	113.84	20.14	>2.74
10i	i-Pr	3-Cl-phenyl	Et	H	COOH	192.16	27.74	>2.27
10j	i-Pr	3-Cl-phenyl	cyclopropyl	H	COOH	162.93	28.03	>1.34
10k	i-Pr	4-Br-phenyl	Me	H	COOH	85.15	23.32	>4.01
10l	i-Pr	4-Br-phenyl	Et	H	COOH	251.16	56.47	1.23
10m	i-Pr	4-Br-phenyl	cyclopropyl	H	COOH	198.56	46.54	1.98
10n	i-Pr	4-I-phenyl	Me	H	COOH	111.03	3.21	2.41
10o	i-Pr	4-I-phenyl	Et	H	COOH	111.04	13.34	1.76
10p	i-Pr	4-F-phenyl	Me	H	COOH	79.17	10.72	2.06
10q	i-Pr	3,4-diCl-phenyl	Me	H	COOH	50.95	23.97	N.T.
10r	i-Pr	4-Cl-phenyl	phenyl	H	COOH	242.71	56.29	1.80
10s	i-Pr	5-Cl-pyridin-2-yl	Et	H	COOH	16.16	8.16	N.T.
10t	cyclobutyl	4-Cl-phenyl	cyclopropyl	H	COOH	88.34	26.09	N.T.
10u	t-butyl	4-Cl-phenyl	Me	H	COOH	2.26	0.19	N.T.
10v	t-butyl	3-Cl-phenyl	Me	H	COOH	5.75	0.53	N.T.
10w	s-butyl	4-Cl-phenyl	Me	H	COOH	175.98	8.01	0.68
10x	s-butyl	4-Cl-phenyl	cyclopropyl	H	COOH	223.73	3.17	0.46
10y	cyclopentyl	4-Cl-phenyl	Me	H	COOH	64.83	9.68	N.T.
10z	cyclopentyl	4-Cl-phenyl	Et	H	COOH	78.21	19.05	N.T.
10aa	cyclopentyl	4-Cl-phenyl	cyclopropyl	H	COOH	76.78	6.14	N.T.
10ab	pentan-3-yl	4-F-phenyl	Me	H	COOH	204.60	6.97	1.45
10ac	pentan-3-yl	4-F-phenyl	Et	H	COOH	250.26	25.79	1.53
10ad	pentan-3-yl	4-Cl-phenyl	Me	H	COOH	182.88	16.71	>3.57
10ae	pentan-3-yl	4-Cl-phenyl	Et	H	COOH	213.36	19.06	1.24
14	i-Pr	4-F-phenyl	H	COOH	Cl	6.21	2.65	N.T.
17	i-Pr	4-F-phenyl	Me	H	$CH_2CH(Et)$ COOH	1.53	0.60	N.T.

Table 1 PPARα transactivation activity of compounds in the present series. HepG2 cells were co-transfected with 4xUAS-tk-luc and pBIND-hPPARα. Transfected cells were treated with the test compounds (1 μM final concentration each), 10 μM fenofibrate, or 0.1% DMSO (*Vehicle*) for 24 h, then used for reporter gene assays. Luciferase activities from reporter plasmids were normalized to *Renilla* luciferase activity. Values are expressed as fold induction as compared to that obtained with

10 μM fenofibrate (*n* = 3).

Next, we investigated the PPAR-subtype selectivity of a representative compound, **10f**.[9] As shown in Figure 2 (A)-2 (C), **10f** selectively induced hPPARα transactivation in a dose-dependent manner, and its EC_{50} value was 0.66 μM, which is lower than that of fenofibrate (EC_{50} = 50 μM). It slightly enhanced hPPARγ transactivation only at the highest concentration (30 μM), and had no effect on hPPARδ (Figure 2 (B), 2(C)). The activity of **10f** towards hPPARα was completely inhibited in the presence of GW6471 (**2**), a hPPARα-specific antagonist,[10] indicating that **10f** induced transcriptional activation of hPPARα by binding to the LBD (Figure 2 (D)).

We then examined the species-selectivity of **10f**, because some PPARα agonists show species-dependent transactivation of PPARα.[11] The classical PPARα agonist pirinixic acid (WY-14643) is more effective on rodent PPARα (rPPARα) than on hPPARα. 5,8,11,14-Eicosatetraynoic acid (ETYA) shows the reverse preference, i.e., it is 10-fold more effective on hPPARα than rPPARα, while fenofibrate does not show apparent species selectivity. We previously demonstrated the importance of the interaction between the distal hydrophobic tail part of our phenylpropanoic acid-type hPPARα agonist and amino acid residue 272 (isoleucine) in the helix-three region of hPPARα LBD for hPPARα-selective activation.[12]

As can be seen from Figure 2 (A), 2 (E), 2 (F), **10f** activated human, mouse and rat PPARα with EC_{50} values of 0.66 μM, 11.27 μM and 15.93 μM, respectively. Thus, **10f** showed species preference for humans, and its transactivation activity was approximately 20-fold less potent in mouse and rat.

In order to examine whether the transactivation of hPPARα elicited by **10f** was mediated directly by the binding of **10f** to the LBD of hPPARα, we evaluated the binding affinity of **10f** to hPPARα LBD. The results of cell-free time-resolved fluorescence resonance energy transfer (TR-FRET) hPPARα competitive binding assay demonstrated that the **10f** indeed binds to hPPARα-LBD, and competitively and dose-dependently displaces Fluormone™ pan-PPAR green as indicated by the reduction in the 518 nm/488 nm ratio; the IC_{50} was 4.48 μM (Figures 2 (G)). On the other hand, a transactivation-inactive compound, **10u**, did not cause any decrease in the 518 nm/488 nm ratio (Figures 2 (H)).

In order to confirm the ability of **10f** to activate genes having a peroxisome proliferator-responsive element (PPRE) in the promoter region at the cellular level, we next examined changes in the expression of a representative hPPARα-mediated gene, the pyruvate dehydrogenase kinase 4 (*PDK4*) gene,[13] in functional liver cell 4 (FLC4) (Figures 2 (I)). Pyruvate dehydrogenase kinase 4 (PDK4) is a key metabolic enzyme, which regulates cell metabolism by inhibiting pyruvate dehydrogenase (PDH). When FLC4 cells were treated with **10f** and then analyzed by means of real-time RT-PCR, we found that *PDK4* mRNA expression was dose-dependently up-regulated. In contrast, cyclophilin A, used as an internal control, was unaffected (data not shown).

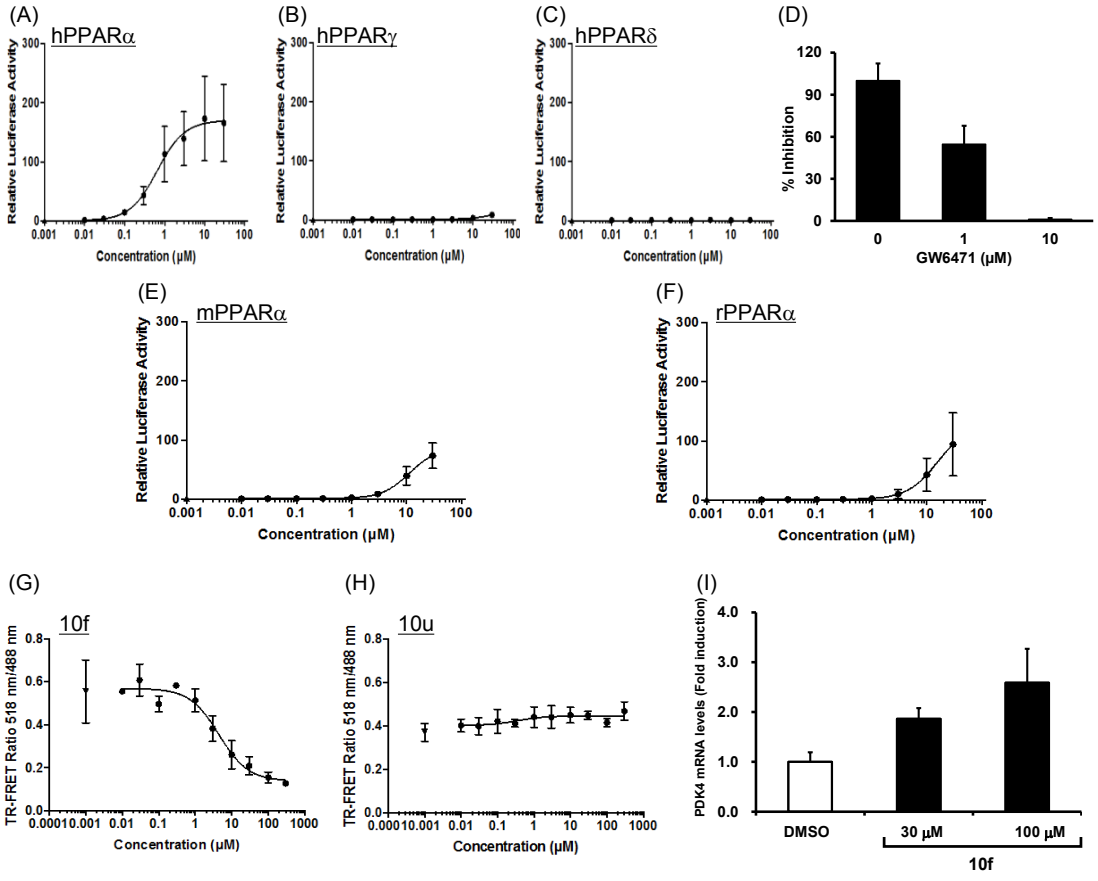

Figure 2. 10f selectively binds to and activates PPARα. Figs 2(A)-2(C). Dose-response relationships for transcriptional activation of GAL4-hPPARα, GAL4-hPPARγ, and GAL4-hPPARδ. HepG2 cells were co-transfected with 4xUAS-tk-luc and pBIND-hPPARα. Transfected cells were treated with **10f** for 24 h, and then used for reporter gene assays. Luciferase activities from reporter plasmids were normalized to *Renilla* luciferase activity. Values are expressed as fold induction compared with the vehicle, set as 1. Fig 2(D). Dose-dependent repression of the transcriptional activation of **10f** by the PPARα antagonist GW6471 (**2**). Cells were pretreated with GW6471 (**2**) for 1 h before addition of **10f** (10 μM final concentration). Percentage inhibition values were calculated based on the activity in the absence of GW6471 (**2**) taken as 100%. Figs 2(E), 2(F). Subtype-selective dose-response relationships for transcriptional activation of GAL4-mPPARα, and GAL4-rPPARα. Figs 2(G), 2(H). Binding affinity assessment of **10f** (active compound) and **10u** (inactive compound) to human PPARα-LBD, evaluated by means of TR-FRET assay. The human PPARα-LBD was incubated with Fluormone™ pan-PPAR green, LanthaScreen™ terbium-labeled anti-GST antibody, and compounds, and the TR-FRET emission ratio (518 nm/488 nm) was measured (*n* = 3). Fig 2(I). **10f** induces the expression of hPPARα target gene. FLC4 cells were treated with various concentrations of **10f** for 48 h. Human *PDK4* mRNA level was measured using real-time RT-PCR and normalized to β2-microglobulin mRNA, set as 1 in the vehicle. Values are expressed as the means ± S.D. (*error*

bars) (*n* = 3).

Based on synthetic considerations (total yield, chirality, physicochemical properties, cost) and potency, we selected **10f** for further studies. Prior to *in vivo* experiments, we confirmed that both **10f** and its sodium salt (**10f Na**)[14] show acceptable *in vitro* ADME profiles (Table 2). Both the molecular form (**10f**) and the ionic form (**10f Na**) exhibited high aqueous solubility and high membrane permeability. They were stable and were recovered almost quantitatively after incubation with both human and mouse liver microsomes. These compounds also showed similar levels of protein binding in human and mouse plasma. Thus, they were considered to be suitable for *in vivo* pharmacological study.

cpd	aqueous solubility[a)]	Caco-2 permeability[b)]	stability[c)]		protein binding[d)]	
	(μM)	(x 10^{-6}cm/s)	human liver microsomes (%)	rat liver microsomes (%)	human plasma (%)	rat plasma (%)
10f	>95	51.8	91	87	99.7	99.0
10f Na	>95	22.5	91	92	99.7	98.9

Table 2 ADME Profiling of 10f a) Solubility in PBS, pH 7.4. b) A–B permeability at 25 μM **10f**. c) Percent (%) remaining after incubation of 0.5 μM **10f** at 37°C for 1h. d) Percent of **10f** bound to protein after incubation of 20 μM **10f** with human or rat plasma at 37°C for 5h. Final DMSO concentration was 0.2%.

To elucidate the *in vivo* effects of **10f** on increased serum triglyceride levels, we used a well-established fructose-fed rat model.[15] After fructose feeding (25% fructose in drinking water) for 3 weeks, serum triglyceride levels of rats fed fructose (25% fructose in drinking water) for 3 weeks were much higher (306 ± 63 mg/dl) than those of rats given normal drinking water (122 ± 26 mg/dl) (Figure 3 (A)). The fructose-fed rats were then administered **10f** or fenofibrate for an additional 2 weeks, together with the fructose. As shown in Figure 3 (B), serum triglyceride levels were lower in rats treated with **10f** or fenofibrate under fructose-feeding conditions than in the vehicle controls after 2 weeks. After the 2-week treatment period, hepatic expression of PPARα target genes, such as acyl-CoA dehydrogenase medium chain (*ACADM*), solute carrier family 25 member 20 (*SLC25A20)*, acyl-CoA Oxidase 1 (ACOX1) and carnitine palmitoyltransferase 1A (*CPT1A*), were enhanced in rats administered **10f** or fenofibrate ((Figures 3 (C)- 3 (F)). These data clearly indicate that the 1*H*-pyrazolo-[3,4-b]pyridine derivative **10f** attenuates hypertriglyceridemia *in vivo*.

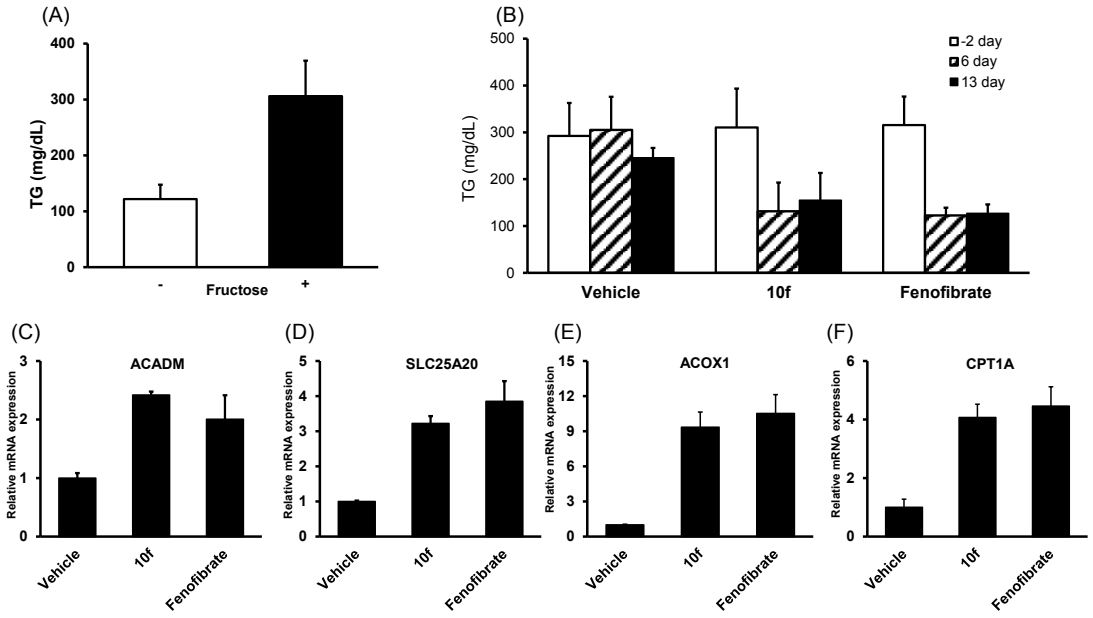

Figure 3. Effect of 10f on *in vivo* lipid metabolism in fructose-fed rats. Fig 3(A) Fructose feeding markedly increased serum triglyceride levels, compared with rats consuming normal drinking water. Male rats received either a 25% fructose challenge in the drinking water or normal drinking

water. Fig 3 (B) Serum triglyceride (*TG*) levels after 2-week oral treatment with **10f** (10 mg/kg/day), fenofibrate (30 mg/kg/day), or 0.5% methylcellulose (*Vehicle*). Three weeks later, fructose-fed rats were orally treated with compound **10f** (10 mg/kg/day), fenofibrate (30 mg/kg/day), or 0.5% methylcellulose (*Vehicle*) for 2 further weeks. Figs 3(C)-3(F). Hepatic mRNA levels of PPARα target genes, *ACADM* (Fig 3(C)), *SLC25A20* (Fig 3(D)), *ACOX1* (Fig 3(E)) and *CPT1A* (Fig 3(F)). mRNA levels in rat liver were measured using real-time RT-PCR and normalized to β2-microglobulin mRNA, set as 1 in the vehicle group. Values are expressed as means ± S.D. (*error bars*) (*n* = 3-5).

In conclusion, we have succeeded in creating a new chemotype of hPPARα-selective activators, as exemplified by **10f**. This confirms that the 1*H*-pyrazolo-[3,4-b]pyridine framework is an attractive basic structure for hPPAR modulators, which are candidate agents to control altered lipid homeostasis, such as dyslipidemia. The SAR results in the current series are somewhat different from those of known fibrate-class hypolipidemic agents. We are currently conducting an X-ray crystallographic study of 1*H*-pyrazolo-[3,4-b]pyridine derivatives complexed with hPPARα LBD to examine the reasons for this difference.

Acknowledgement.

This work was supported in part by a grant for Platform for Drug Discovery, Informatics, and Structural Life Science from the Ministry of Education, Culture, Sports, Science and Technology, Japan, the Japan Agency for Medical Research and Development (AMED) under Grants JP18am0101085, Platform Project for Supporting Drug Discovery and Life Science Research (Basis for Supporting Innovative Drug Discovery and Life Science Research

(BINDS)) from AMED under Grant Number JP19am0101085, JSPS KAKENHI (grant numbers 15H02896, 16K13044 and 18H03190), and Takeda Science Foundation. The authors gratefully thank Advanced Science Research Center, Okayama University for the single crystal XRD measurements.

References and Notes

1. Varga, T.; Czimmerer, Z.; Nagy, L. *Biochim. Biophys. Acta.* **2011**, *1812*, 1007.

2. Philippe, L.; Giulia, C.; Jean-Charles, F.; Bart, S. *J. Clin. Invest.* **2006**, *116*, 571.

3. Issemann, I.; Prince, R. A.; Tugwood, J. D. Green, S. *J. Mol. Endocrinol.* **1993**, *11*, 37.

4. Ban, S.; Kasuga, J.; Nakagome, I.; Nobusada, H.; Takayama, F.; Hirono, S.; Kawasaki,H.; Hashimoto, Y.；Miyachi, H. *Bioorg. Med. Chem.* **2011**, *15,* 3183.

5. Araya, Y.; Kasuga, J.; Toyota, K.; Hirakawa, Y.; Oyama, T.; Makishima, M.; Morikawa, K.; Hashimoto, Y.；Miyachi, H. *Chem. Pharm. Bull. (Tokyo).* **2008**, *56*, 1357.

6. Kuwabara, N.; Oyama, T.; Tomioka, D.; Ohashi, M.; Yanagisawa, J.; Shimizu, T.; Miyachi,

H. *J. Med. Chem.* **2012**, *55*, 893.

7. Tachibana, K.; Yuzuriha, T.; Tabata, R.; Fukuda, S.; Maegawa, T.; Takahashi, R.; Tanimoto, K.; Tsujino, H.; Nunomura, K.; Lin, B.; Matsuura, Y.; Tanaka, T.; Hamakubo, T.; Sakai, J.;Kodama, T.; Kobayashi, T.; Ishimoto, K.; Miyachi, H.; Doi, T. *J. Biol. Chem.* **2018**, *293*, 10333.

8. Nolte, R.T.; Wisely, G. B.; Westin, S.; Cobb, J. E.; Lambert, M. H.; Kurokawa, R.; Rosenfeld, M. G.; Willson, T. M.; Glass, C. K.; Milburn, M. V. *Nature.* **1998**, *395*, 137.

9. Physico-chemical properties of compound **10f**: ^{1}H-NMR (300 MHz, DMSO-d_6) δ 8.31,(2H, *dd*, J=6.8, 2.1Hz), 7.56,(1H, *s*), 7.47,(2H, *dd*, J=6.9, 2.2Hz), 3.86,(1H, *sep*, J=6.8Hz), 2.76,(3H, s), 1.42,(6H, *d*, J=6.7Hz). ^{13}C-NMR (100 MHz, DMSO-d_6) δ 167.27, 159.11, 151.12, 151.04, 137.95, 135.63, 129.52, 128.99, 121.83, 117.60, 109.29, 27.41, 24.45, 21.96. MS 329 $(M+H)^{+}$. mp. 270.6-271.4 ºC . HPLC purity was estimated to be 99.5% by means of reversed-phase HPLC, using a Pegasil ODS sp100 column (4.6 mm x 250 mm, Senshu Chemical, Japan) fitted on a JASCO HPLC system, with CH_3CN : 0.1% TFA = 2:1 v/v as the eluent and detection at 254 nm.

10. Xu, H. E.; Stanley, T. B.; Montana, V. G.; Lambert, M. H.; Shearer, B. G.; Cobb, J. E.; McKee, D. D.; Galardi, C. M.; Plunket, K. D.; Nolte, R. T.; Parks, D. J.; Moore, J. T.; Kliewer, S. A.; Willson, T. M.; Stimmel, J. B. *Nature.* **2002**, *415*, 813.

11. Keller, H.; Devchand, P. R.; Perround, M.; Wali, W. *Biol. Chem*, **1997**, *378*, 651.

12. Miyachi, H.; Uchiki, H. *Bioorg. Med. Chem. Lett.* **2003,** *13*, 3145.

13. Raza-Iqbal, S.; Tanaka, T.; Anai, M.; Inagaki, T.; Matsumura, Y.; Ikeda, K.; Taguchi, A.;

Gonzalez, F. J.; Sakai, J.; Kodama, T. *J. Atheroscler. Thromb.* **2015**, *22*, 754.

14. Physico-chemical properties of compound **10fNa**: ^{1}H-NMR (300 MHz, $CDCl_3$) δ 8.32,(2H, *dd*, J=6.9, 2.2Hz), 7.48,(2H, *dd*, J=7.0, 2.3Hz), 7.08,(1H, *s*), 3.78,(1H, *sep*, J=6.9Hz), 2.65,(3H, *s*), 1.40,(6H, *d*, J=6.9Hz). mp. >300 ºC . HPLC purity was estimated to be 99.8% by means of reversed-phase HPLC, using a Pegasil ODS sp100 column (4.6 mm x 250 mm, Senshu Chemical, Japan) fitted on a JASCO HPLC system, with CH_3CN : 0.1% TFA = 2:1 v/v as the eluent and detection at 254 nm.

15. Park, J.; Lemieux, S.; Lewis, G. F.; Kuksis, A.; Steiner, G. *J. Lipid Res.* **1997**, *38*, 2529.

Graphical Abstract

Structural development studies of a series of 1*H*-pyrazolo-[3,4-b]pyridine-4-carboxylic acid human peroxisome proliferator-activated receptor (PPAR) α-selective agonists

Hiroyuki Miyachi, Tomohiro Yuzuriha, Ryotaro Tabata, Syohei Fukuda, Kazuto Nunomura, Bangzhong Lin, Tadayuki Kobayashi, Kenji Ishimoto, Takefumi Doi, Keisuke Tachibana

Leave this area blank for abstract info.